Chapter 4

The Effect of Elastic Softening and Cooperativity on the Fragility of Glass-Forming Metallic Liquids

Key words: Amorphous metals, Shear transformation zones, Ultrasonic measurement, Compression test, Viscosity

4.1 Abstract

Viscosity and isoconfigurational shear modulus data *G*, from the literature and current experiments, were analyzed for strong and fragile liquids. A recently developed Cooperative Shear Model was utilized to fit the viscosity of the different glasses. The relative effects of the "elastic" and "cooperative volume" fragility indices were observed to be equivalent in regards to the softening of the shear flow barrier. This equivalence gives rise to a factor of $\sim G^2$ in the softening of the shear flow barrier used in the Cooperative Shear Model.

4.2 Introduction

The concept of fragility was first introduced by Angell to facilitate the comparison of the rheology of different liquids [1]. Furthermore, Angell introduced a fragility parameter $m = \partial \log \eta / \partial \left(T/T_g\right)_{Tg}$ to describe the decrease of η with T. In this description, fragility measures the degree of deviation of viscosity or relaxation time of a glass-forming liquid from Arrhenius behavior [2-4]. For strong liquids, m is small (m ~ 15–25) and an Arrhenius behavior is closely followed. The viscosity of fragile liquids decreases more rapidly with T than an Arrhenius fitting would predict and m ranges up to ~ 100. This concept of fragility has been applied to a variety of different systems, including silicate glasses, organic glasses, and metallic glasses. Furthermore, the fragility of a liquid may be analyzed in terms of the thermodynamics or kinetics of the liquid.

The thermodynamic fragility is assessed by using the excess (or configurational) entropy of the liquid referenced to the crystalline state and the excess entropy of the liquid at the glass transition temperature [3-5]. When the thermodynamic fragilities are examined over the entire range of fragilities there are a few anomalies. SiO_2 is known to be an extremely strong liquid, but when the thermodynamic fragility is assessed, the resulting fragility is far lower than expected from rheological data. Additional anomalies have been identified in several polymers. According to Angell these anomalies would not have arisen had the entropies been assessed by an all-liquid route, as used in MD computer simulations [3]. The problems that arise with evaluating the thermodynamic fragility (due to it being referenced to the crystalline state) do not arise in determining the kinetic fragility, as it is an entirely liquid state property [3]. Only the glass transition temperature is referenced in evaluating the kinetic fragility resulting in a complete

decoupling of the crystalline phase and melting temperature from the results (see the equation for m above). Therefore, in the present study, we will confine our work to the kinetic fragility of the material.

Various explanations have been put forward to explain fragility in liquids. One such model is the defect diffusion model, in which the difference between a fragile and strong liquid is described in terms of the tendency for the liquid to form clusters of defects instead of isolated defects [6, 7]. It has also been theorized that first-order transitions and the spatial range scale of interactions can be used to describe fragilities [8]. One of the more cited approaches involves Potential Energy Landscape theory [3-5, 9, 10] In this theory the shear flow barrier height, distribution, and curvature all lead to a liquid being either more or less fragile.

In recent studies [11-13], it has been shown that plastic yielding in metallic glasses can be effectively accounted for by adopting a cooperative shear yielding analysis for flow similar to the one developed by Frenkel [14] for determining the shear strength of dislocation-free crystals. In the present study, we employ that analysis to investigate the fragility of glass-forming liquids.

4.3 Experimental

A $La_{55}Al_{25}Ni_5Cu_{10}Co_5$ glass was utilized as one of the glasses in the fragility analysis [15]. The alloy ingot was prepared by arcmelting La, Al, Ni, Cu, and Co together under a titanium gettered argon atmosphere. The alloy was then cast into 4 mm diameter rods, and the amorphous nature was verified by thermal analysis and x-ray diffraction. The rods were cut and polished to form 4 mm tall cylindrical specimens.

We measured the temperature-dependent equilibrium isoconfigurational shear modulus of the liquid by performing ultrasonic measurements on thermally relaxed specimens annealed at temperatures between 437 K and 457 K in the vicinity of T_g**.** Shear wave speeds were measured using the pulse-echo overlap setup described in Ref. [13]. Densities were measured by the Archimedes method, as given in the American Society for Testing and Materials standard C693-93. Measurements were performed *ex situ* on the amorphous specimens at room temperature, after they were quenched rapidly from the annealing temperature. The quenching process was done in liquid nitrogen to avoid oxidation of the specimen. The isoconfigurational shear moduli at the annealing temperatures were then estimated by extrapolating the room temperature measurements using a linear Debye-Grüneisen constant, $(dG/dT)_{Glass}$, to account for the thermal expansion effect on the shear modulus of the frozen glass. A dimensional analysis was used to estimate the Debeye-Grüneisen coefficient of $La_{55}Al_{25}Ni_5Cu_{10}Co_5$. The Debye-Grüneisen coefficient of $Zr_{46.75}Ti_{8.25}Cu_{7.5}Ni_{10}Be_{27.5}$ was experimentally determined to be 9 MPa/K. The glass transition temperature was taken as the temperature where the liquid viscosity is 10^{12} Pa s and was found to be 439.1 K and 586.3 K for $La_{55}Al_{25}Ni_5Cu_{10}Co_5$ and $Zr_{46.75}Ti_{8.25}Cu_{7.5}Ni_{10}Be_{27.5}$, respectively. The shear modulus at the glass transition

temperature is 14.5 for $La_{55}Al_{25}Ni_5Cu_{10}Co_5$ and 34.82 for $Zr_{46.75}Ti_{8.25}Cu_{7.5}Ni_{10}Be_{27.5}$. The Debye-Grüneisen coefficient for $La_{55}Al_{25}Ni_5Cu_{10}Co_5$ can then be estimated using:

$$DG_{La} = DG_{Vit4} \frac{T_{gVit4}}{T_{gLa}} \frac{G_{La}}{G_{Vit4}}$$

where DG is the Debye-Grüneisen coefficient, T_g is the glass transition temperature, and G is the isoconfigurational shear modulus at the glass transition temperature. From this the Debye-Grüneisen coefficient for $La_{55}Al_{25}Ni_5Cu_{10}Co_5$ is 5.07 MPa/K.

The viscosity data used in this chapter may be found in Chapters 2–3 and in Refs. [3, 16-20]. In addition to the data from the $La_{55}Al_{25}Ni_5Cu_{10}Co_5$ alloy, the isoconfigurational shear modulus data used in the preparation of the figures shown in the present chapter are taken from Chapters 2–3 and Refs. [13, 21-23]. The G data for $La_{55}Al_{25}Ni_5Cu_{10}Co_5$ is shown in Fig. 4.8.

For a more complete description of the experimental methods used please refer to Chapter 2.3.

4.4 Discussion

In several recent studies [11-13], a thermodynamic link between the isoconfigurational shear modulus, G, and viscosity η has been proposed. Figures 1–7 show the fits obtained for the different glasses using the model developed in those studies and later modified in Chapter 2.

$$\frac{\eta_e}{\eta_\infty} = \exp\left\{\frac{T_g}{T}\ln\left(\frac{\eta_g}{\eta_\infty}\right)\exp\left[(n+p)\left(1-\frac{T}{T_g}\right)\right]\right\}. \tag{4.1}$$

In this equation η_e is the equilibrium viscosity, η_∞ is the viscosity of the liquid at the plank limit, T_g is the glass transition temperature as defined at a viscosity of 10^{12} Pa s, η_g is the viscosity at the glass transition, and T is the temperature of the experiment. The fitting parameters n and p are the reduced "elastic" and "cooperative volume" fragility indices, respectively, which quantify the contributions of isoconfigurational shear modulus and cooperative shear volume to the softening of the shear flow barrier. A more detailed description of this model is given in Chapter 2. The viscosity data were fit using the combined factor of $(n+p)$. The fits were done both for strong and fragile liquids. The materials analyzed included O-terphynol, $Pt_{57.2}Ni_{5.3}Cu_{14.7}P_{22.5}$, $Pd_{43}Ni_{10}Cu_{27}P_{20}$, Glycerol, $La_{55}Al_{25}Ni_5Cu_{10}Co_5$, $Zr_{46.75}Ti_{8.25}Cu_{7.5}Ni_{10}Be_{27.5}$, and SiO_2. Over this wide range of fragility the model was found to accurately predict the variations in viscosity with respect to temperature.

It is possible to directly determine n by fitting the liquid shear modulus data using

$$G(T) = G_g \exp\left[n\left(1-\frac{T}{T_g}\right)\right] \tag{4.2}$$

where T is the temperature of the experiment, G(T) is the equilibrium isoconfigurational shear modulus at temperature T, and G_g is the shear modulus at T_g. The shear modulus data from the present experiments and available data from the literature were fit with Eq. 4.2.

In Table 4.1 physical parameters such as T_g and $G(T_g)$ are presented alongside the fitting parameters used for fitting the viscosity and isoconfigurational shear modulus data. Furthermore, p was determined for each glass using the "n" determined by fitting the measured isoconfigurational shear modulus data and subtracting from the collective term "$(n+p)$" obtained by fitting the viscosity data. The relative effects of shear modulus and STZ size Ω on the flow properties of the material are quantified by the term q:

$$q = \frac{n}{n+p}. \tag{4.3}$$

The average q for the different glasses is $q = 0.466$, with relatively small differences among the materials. Hence, the effects on flow of elastic fragility and cooperativity are nearly equivalent. From this, it becomes apparent that $n \approx p$. From the derivation shown in Chapter 2, this results in the barrier height controlling flow "softening" with a factor of $\sim G^2$. This leads to a new version of Eq. 4.1:

$$\frac{\eta_e}{\eta_\infty} = \exp\left\{\frac{T_g}{T}\ln\left(\frac{\eta_g}{\eta_\infty}\right)\exp\left[2n\left(1-\frac{T}{T_g}\right)\right]\right\}. \tag{4.4}$$

	T_g (K)	G_g (GPa)	n+p	n_G	p_G	q
O-Terphenyl	239.2	1.69	5.104	2.959	2.145	0.580
$Pt_{57.2}Ni_{5.3}Cu_{14.7}P_{22.5}$	489.2	30.5	2.699	1.275	1.424	0.472
$Pd_{43}Ni_{10}Cu_{27}P_{20}$	568.9	30.3	2.491	1.295	1.196	0.520
Glycerol	182	4.62	2.084	0.803	1.281	0.386
$La_{55}Al_{25}Ni_5Cu_{10}Co_5$	439.1	14.5	1.143	0.567	0.576	0.496
$Zr_{46.75}Ti_{8.25}Cu_{7.5}Ni_{10}Be_{27.5}$	586.3	34.82	1.142	0.602	0.539	0.528
SiO_2	1468	35.4	0.217	0.061	0.156	0.282

Table 4.1. Physical parameters and fits for the listed glasses. T_g is the glass transition temperature as defined at 10^{12} Pa-s. G_g is the isoconfigurational shear modulus at T_g. $(n+p)$ is the combined effect of the "elastic" and "cooperative volume" fragilities as determined using Eq. 4.1. The parameter n_G is the elastic fragility index as determined from the isoconfigurational shear modulus and eq. 4.2. The parameter p_G is found using $(n+p)-n_G$ and is the cooperative volume fragility index part of $(n+p)$. The quantity q is a measure of the relative influence of the elastic and cooperative volume fragilities, and is quantified as $q = n_G/(n+p)$.

Using Eq. 4.4 and the n obtained by fitting the shear modulus data for the different glasses, one can fit the liquid viscosity with the single independent parameter "2n." Those fits are seen in Figs. 4.1–4.7 as the dashed lines. The shear modulus data itself was converted into viscosity using the inverse of Eq. 4.1:

$$\eta = \eta_g \exp\left[\frac{T_g}{T}\left(\frac{G}{G_g}\right)^q\right]. \tag{4.5}$$

G_g and $\eta_g = 10^{12}$ Pa-s are the isoconfigurational shear modulus and viscosity of the undercooled liquid at the glass transition temperature. The data for G are then converted into predicted viscosity using Eq. 4.5 and $q \approx 0.5$. The converted G data is then plotted with the measured viscosity data in Figs. 4.1–4.7. The original G data for $La_{55}Al_{25}Ni_5Cu_{10}Co_5$ is supplied in Fig. 4.8.

The best agreement between the converted shear modulus data and the viscosity data is seen in the metallic glasses. While there is reasonable agreement for the other glasses there is a deviation from the $q \approx 0.5$ behavior. This is very likely due to the more complex interactions inherent in the different glasses presented. The bonding in the metallic glasses will be the closest to that expected for centrosymmetric atomic pair interactions. The organic glasses and SiO_2 will have more complex interactions due to their molecular structures and covalent/directional bonding. Therefore, it is possible that the differences in bonding affect the relative weighting of the elastic and cooperative volume fragility indices. The discrepancy in q may also be due to the method by which the shear modulus data was obtained for the organic and silicate glasses. Brillioun scattering was used to measure the shear modulus data, and since this is a dynamic process it is probable that the data does not correspond to quasi-static equilibrium states. Even so there is good agreement for all of the liquids studied, and from the present study it would appear that for simple liquids the elastic and cooperative volume fragility indices governing the softening of the shear flow barrier are approximately equivalent.

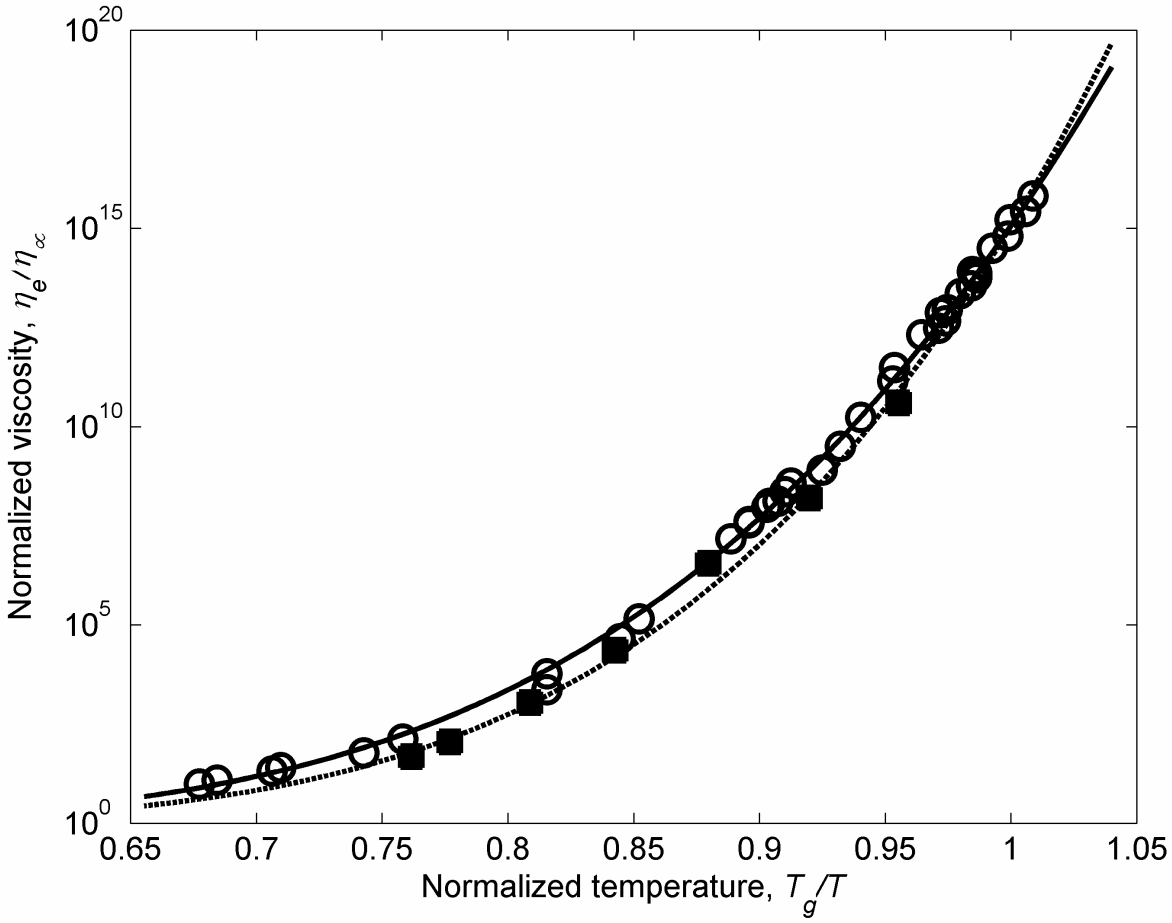

Figure 4.1. (○) O-Terphenyl Newtonian viscosity data. (■) O-Terphenyl viscosity predicted from shear modulus data (corrected for Debye-Grüneisen effect) using Eq. (4.5). The solid line is a prediction from Eq. (4.1) using (n + p), and the dashed line is a prediction from Eq. (4.4) using n_G.

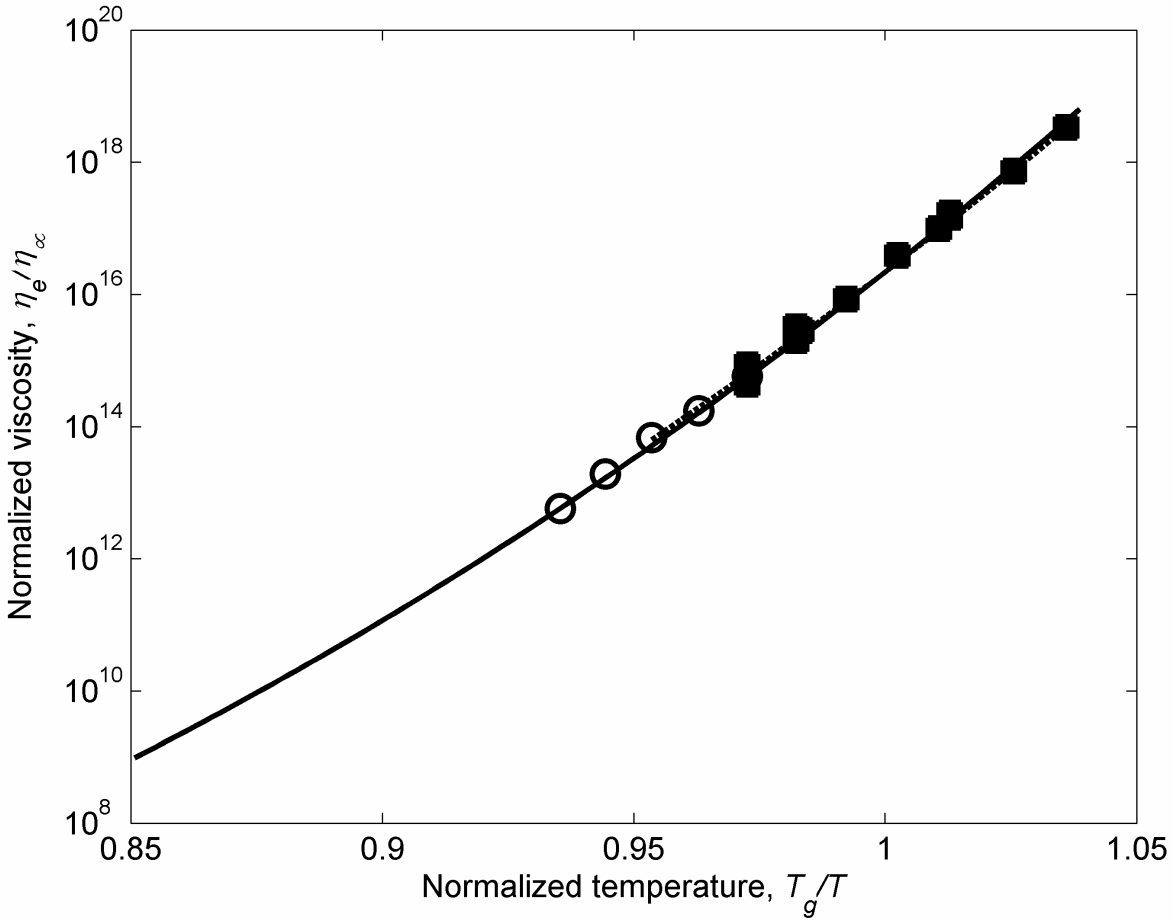

Figure 4.2. (○) $Pt_{57.2}Ni_{5.3}Cu_{14.7}P_{22.5}$ Newtonian viscosity data. (■) $Pt_{57.2}Ni_{5.3}Cu_{14.7}P_{22.5}$ viscosity predicted from shear modulus data (corrected for Debye-Grüneisen effect) using Eq. (4.5). The solid line is a prediction from Eq. (4.1) using (n + p), and the dashed line is a prediction from Eq. (4.4) using n_G.

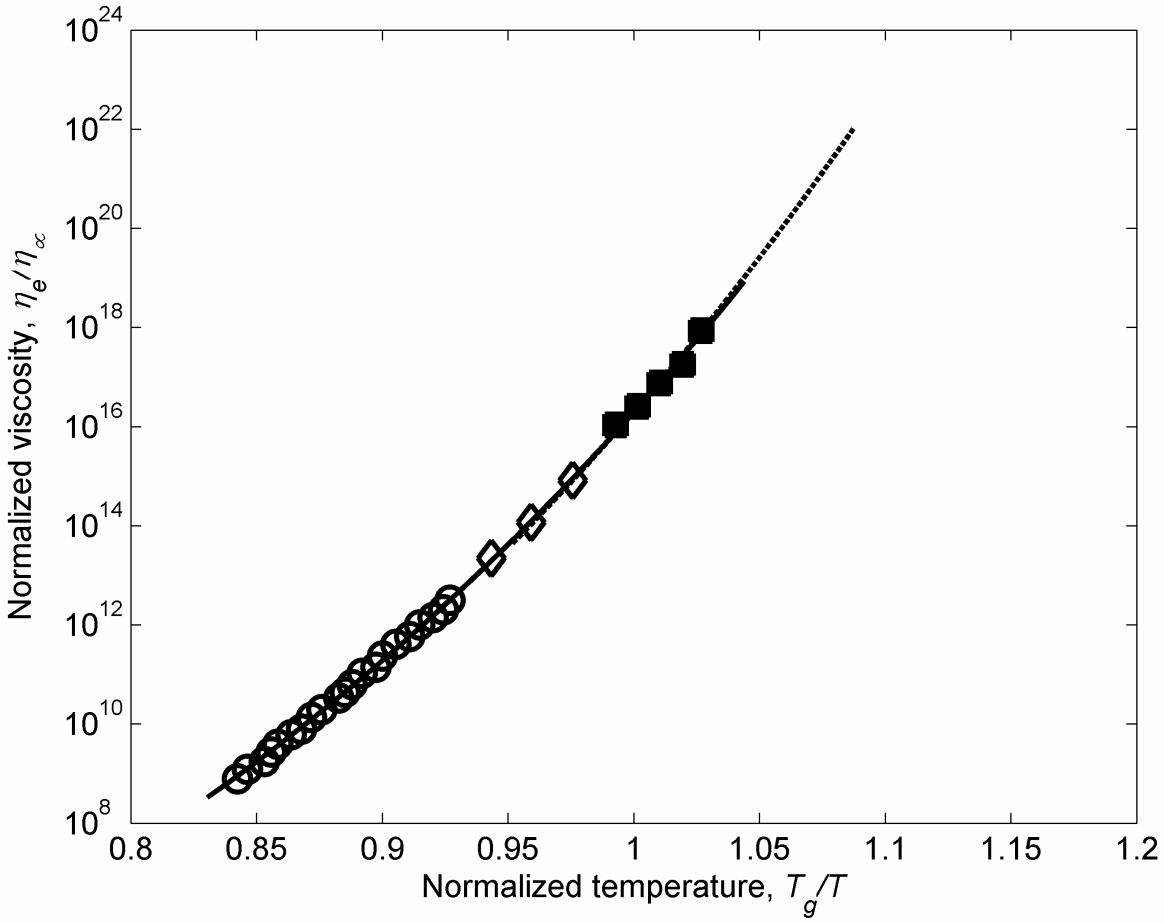

Figure 4.3. $Pd_{43}Ni_{10}Cu_{27}P_{20}$ Newtonian viscosity data from (○) Ref. [17] and (◊) experiments. (■) $Pd_{43}Ni_{10}Cu_{27}P_{20}$ viscosity predicted from shear modulus data (corrected for Debye-Grüneisen effect) using Eq. (4.5). The solid line is a prediction from Eq. (4.1) using (n + p), and the dashed line is a prediction from Eq. (4.4) using n_G.

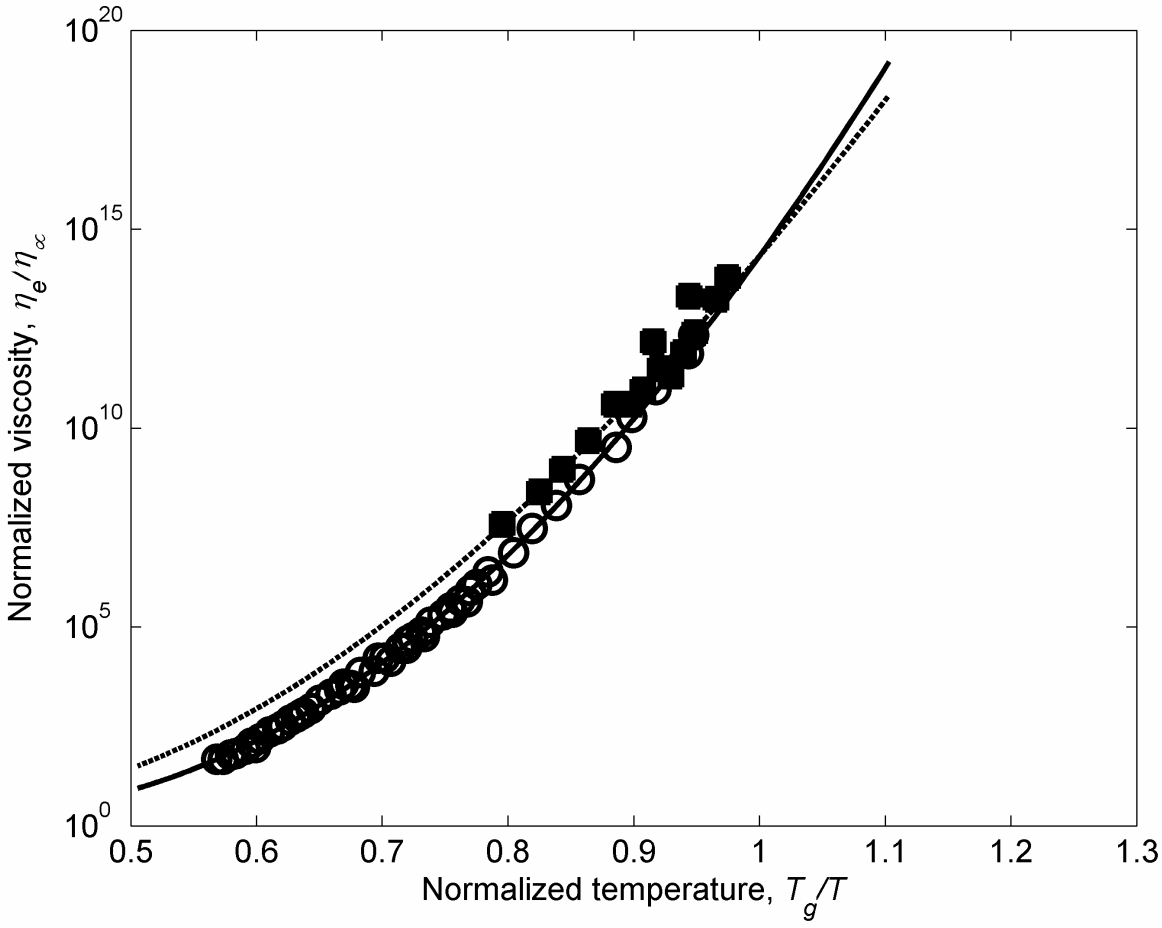

Figure 4.4. (○) Glycerol Newtonian viscosity data. (■) Glycerol viscosity predicted from shear modulus data (corrected for Debye-Grüneisen effect) using Eq. (4.5). The solid line is a prediction from Eq. (4.1) using (n + p), and the dashed line is a prediction from Eq. (4.4) using n_G.

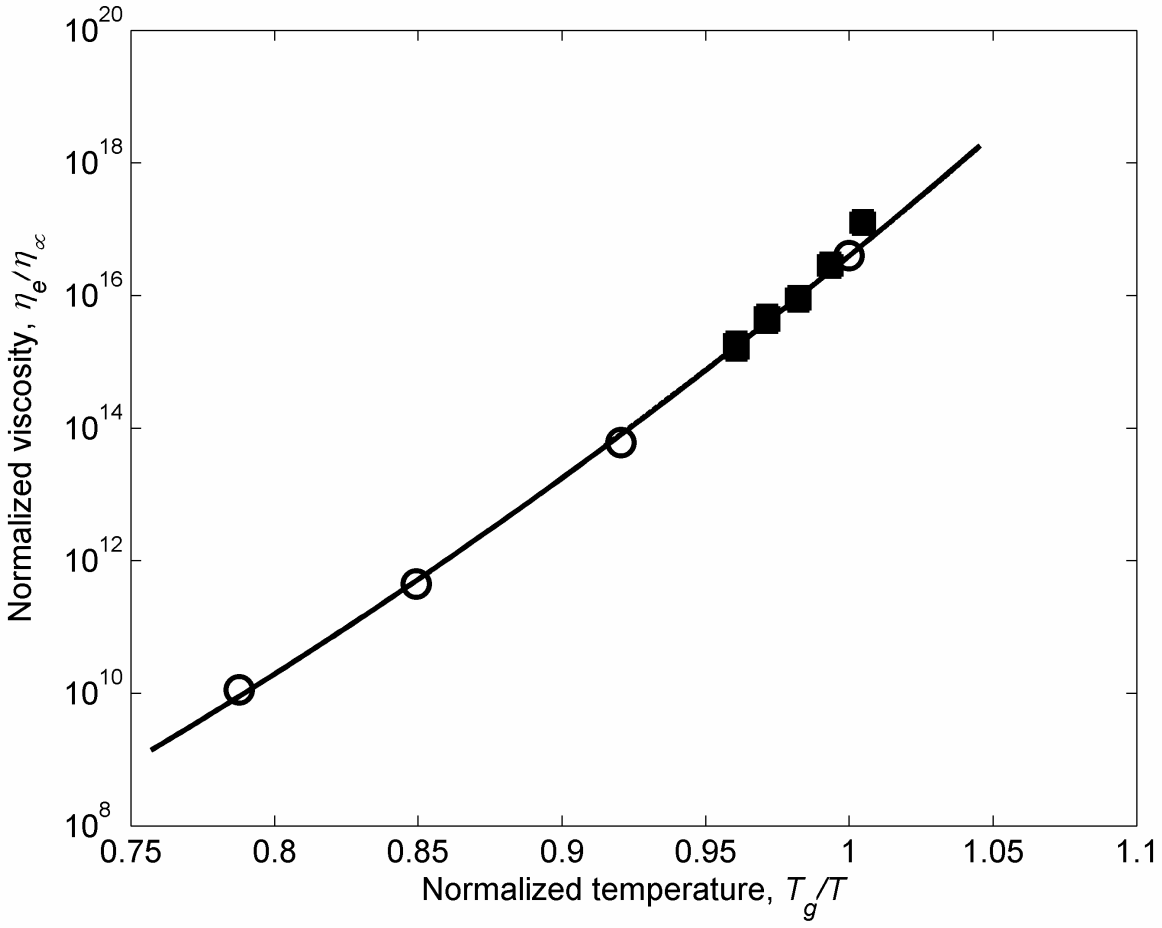

Figure 4.5. (○) $La_{55}Al_{25}Ni_5Cu_{10}Co_5$ Newtonian viscosity data. (■) $La_{55}Al_{25}Ni_5Cu_{10}Co_5$ viscosity predicted from shear modulus data (corrected for Debye-Grüneisen effect) using Eq. (4.5). The solid line is a prediction from Eq. (4.1) using (n + p), and the dashed line is a prediction from Eq. (4.4) using n_G.

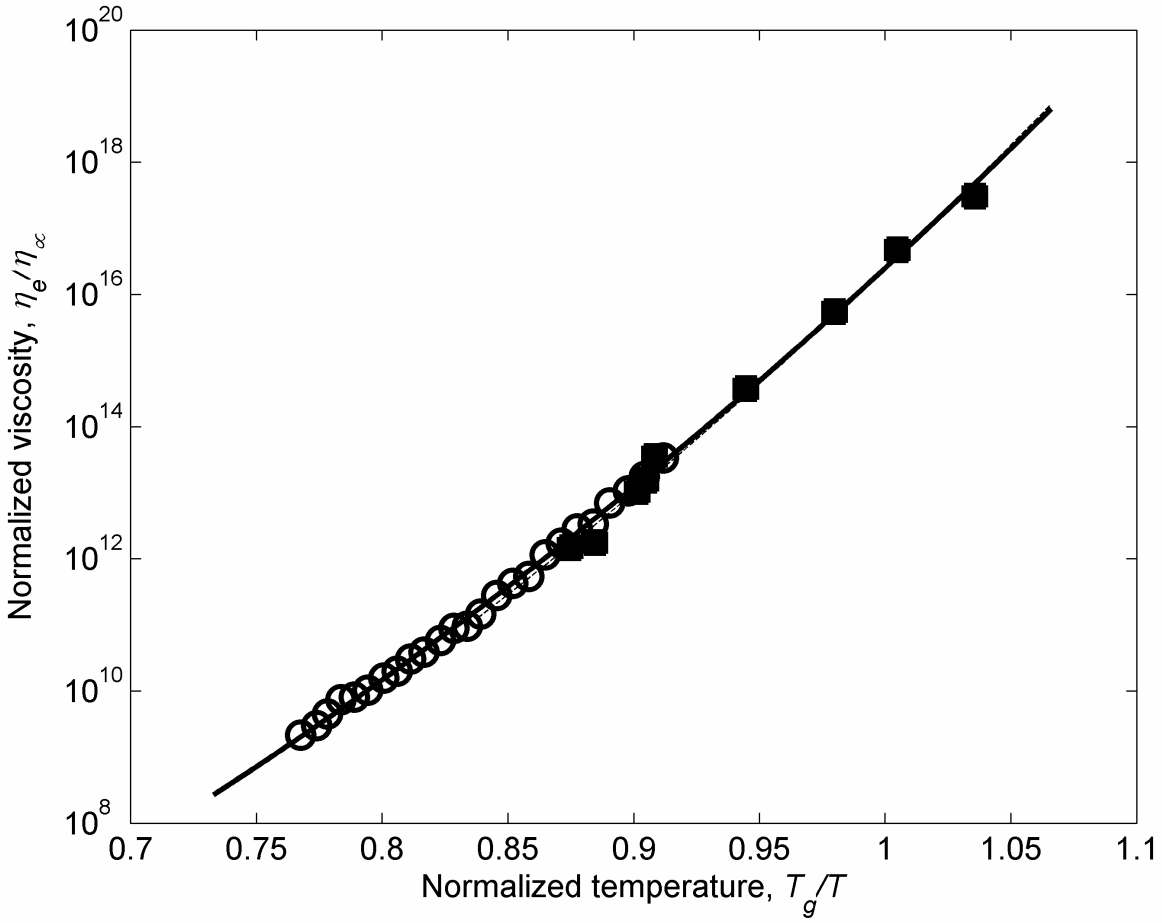

Figure 4.6. (○) $Zr_{46.75}Ti_{8.25}Cu_{7.5}Ni_{10}Be_{27.5}$ Newtonian viscosity data. (■) $Zr_{46.75}Ti_{8.25}Cu_{7.5}Ni_{10}Be_{27.5}$ viscosity predicted from shear modulus data (corrected for Debye-Grüneisen effect) using Eq. (4.5). The solid line is a prediction from Eq. (4.1) using (n + p), and the dashed line is a prediction from Eq. (4.4) using n_G.

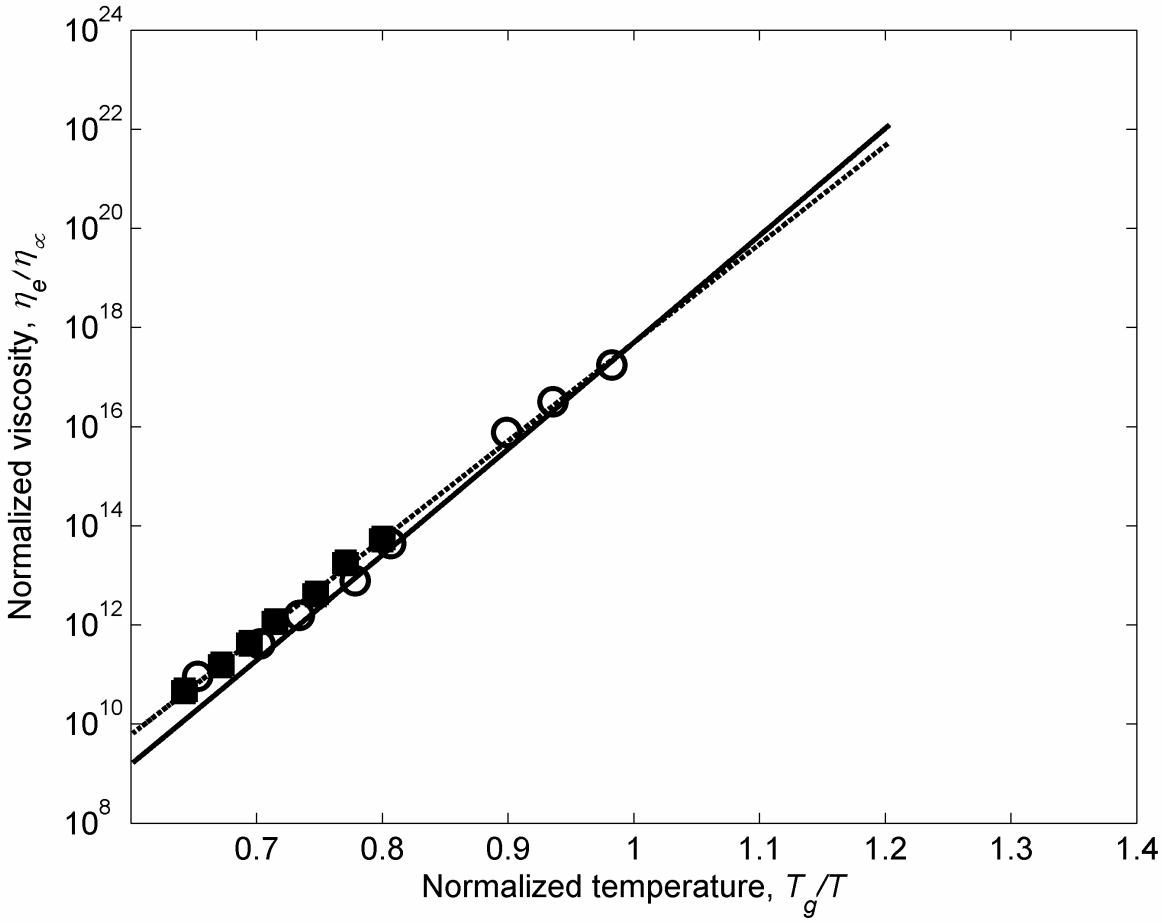

Figure 4.7. (○) SiO_2 Newtonian viscosity data. (■) SiO_2 viscosity predicted from shear modulus data (corrected for Debye-Grüneisen effect) using Eq. (4.5). The solid line is a prediction from Eq. (4.1) using (n + p), and the dashed line is a prediction from Eq. (4.4) using n_G.

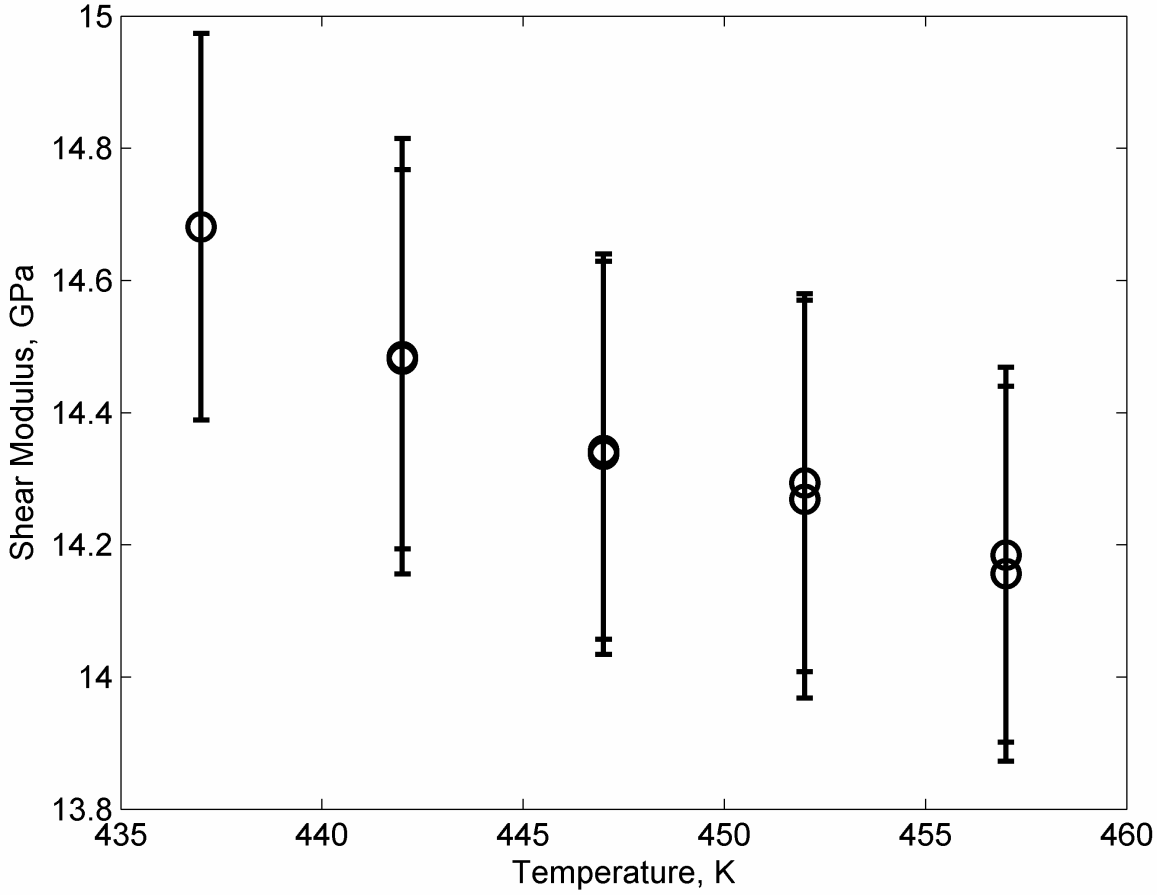

Figure 4.8. Isoconfigurational shear modulus versus annealing temperature for $La_{55}Al_{25}Ni_5Cu_{10}Co_5$

4.5 Conclusion

In conclusion, viscosity and isoconfigurational shear modulus data from the literature and current experiments was analyzed. This study utilized fragile to strong liquids and included organic, metallic, and silicate glasses. A recently developed cooperative shear model [11] was utilized to fit the viscosity of the different glasses. The elastic and cooperative volume fragility indices were used to describe the softening of the shear flow barrier. Furthermore, the "elastic" fragility index was experimentally determined by fitting the isoconfigurational shear modulus behavior versus temperature.

By looking at the combined fragility indices and the experimentally determined elastic fragility index it was possible to correlate the relative influence of the separate indices on the flow softening of the material. It was determined empirically that the elastic and cooperative volume fragility indices are equivalent. Due to this equivalence a factor of $\sim G^2$ may be attributed to the softening of the shear flow barrier used in the Cooperative shear model. The viscosity fits obtained using this conclusion were compared to the fits obtained directly from the Cooperative Shear Model. The best agreement between the two fits was observed in the metallic glasses. While the fits for the other glasses were adequate, there was some deviation between the two methods. This can be contributed to the more complex interactions found in the organic and silicate glasses giving rise to differences in the relative influence of the elastic and cooperative volume fragilities. Therefore, in simple liquids the elastic and cooperative volume fragilities may be assumed to be equivalent in their effect on the softening of the shear flow barrier.

4.6 References

[1] C. A. Angell, Relaxations in Complex Systems, Springfield, VA 22161: National Technical Information Service, U.S. Department of Commerce (1985).

[2] G. J. Fan, and E. J. Lavernia, Phil. Mag. 84, 2471 (2004).

[3] L.-M. Martinez, and C. A. Angell, Nature 410, 663 (2001).

[4] C. A. Angell, J. Res. Natl. Inst. Stand. Technol. 102, 171 (1997).

[5] G. J. Fan, H. Choo, and P. K. Liaw, J. Non-Crystalline Solids 351, 3879 (2005).

[6] J. T. Bendler, J. J. Fontanella, and M. F. Shlesinger, J Chem. Phys. 118, 6713 (2003).

[7] J. T. Bendler, J. J. Fontanella, and M. F. Shlesinger, J Non-Crystalline Solids 352, 4835 (2006).

[8] X. Xia, and P. G. Wolynes, Proceedings of the National Academy of Sciences 97, 2990 (2000).

[9] S. Sastry, Nature 409, 164 (2001).

[10] L. Hu, X. Bian, W. Wang, G. Liu, and Y. Jia, J. Phys. Chem. B 109, 13737 (2005).

[11] W. L. Johnson, and K. Samwer, Phys Rev. Lett. 95, 195501 (2005).

[12] M D Demetriou, J S Harmon, M Tao, G Duan, K Samwer, and W L Johnson, Phys. Rev. Lett. 97, 065502 (2006).

[13] M. L. Lind, G. Duan, and W. L. Johnson, Phys. Rev. Lett. 97, 015501 (2006).

[14] J. Frenkel, Z. Phys. 37, 572 (1926).

[15] Z. P. Lu, H. Tan, and Y. Li, Mat. Tran. JIM 41, 1397 (2000).

[16] J Lu, Ph.D. Thesis. Pasadena: California Institute of Technology (2002).

[17] G. H. Fan, H.-J. Fecht, and E. J. Lavernia, Appl. Phys. Lett. 84, 487 (2004).

[18] Z. Lu, Y. Li, and C. T. Liu, J Applied Phys. 93, 286 (2003).

[19] K. Rah, and B. C. Eu, Phys. Rev. E 68, 051204 (2003).

[20] I. V. Blazhnov, N. P. Malomuzh, and S. V. Lishchuk, J Chem. Phys. 121, 6435 (2004).

[21] C. Dreyfus, A. Aouadi, J. Gapinski, M. Matos-Lopes, W. Steffen, A. Patkowski, and R. M. Pick, Phys. Rev. E 68, 011204 (2003).

[22] F. Scarponi, L. Comez, D. Fioretto, and L. Palmieri, Phys. Rev. B 70, 054203 (2004).

[23] A. Polian, D. Vo-Thanh, and P. Richet, Europhys. Lett. 57, 375 (2002).